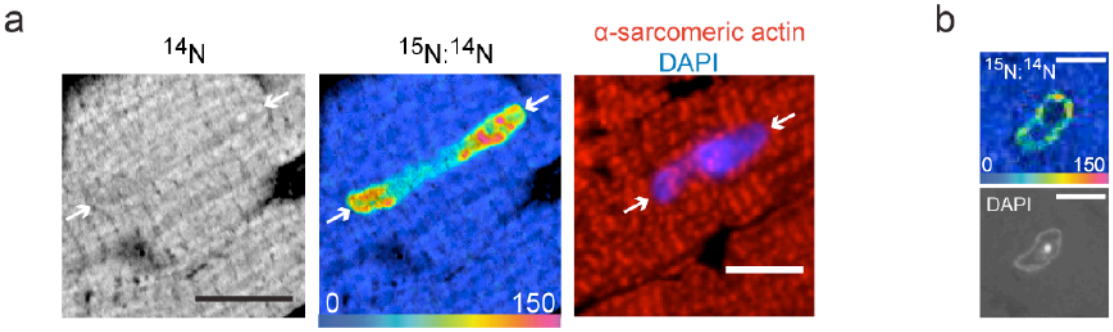

Figure S1: MIMS imaging of cardiomyocytes in cardiac tissue sections.

a) ^{15}N-thymidine labeled cardiomyocyte. Left: ^{14}N mass image demonstrating periodic sarcomeric structures. Middle: ^{15}N:^{14}N Hue Saturated Image (HSI) image demonstrating ^{15}N-labeled nucleus (white arrows). Right: Adjacent section stained for α-sarcomeric actin demonstrating sarcomeric structures surrounding nucleus. Scale bar=10μm.

b) ^{15}N-thymidine labeling in cardiomyocyte nuclei tends to be most intense at the periphery of the nucleus (top image: ^{15}N:^{14}N HSI) in a pattern similar to DAPI staining (bottom image). Similar patterns of chromatin condensation at the periphery of cardiomyocyte nuclei have also been observed in studies using electron microscopy[1]. Scale bar = 5μm.

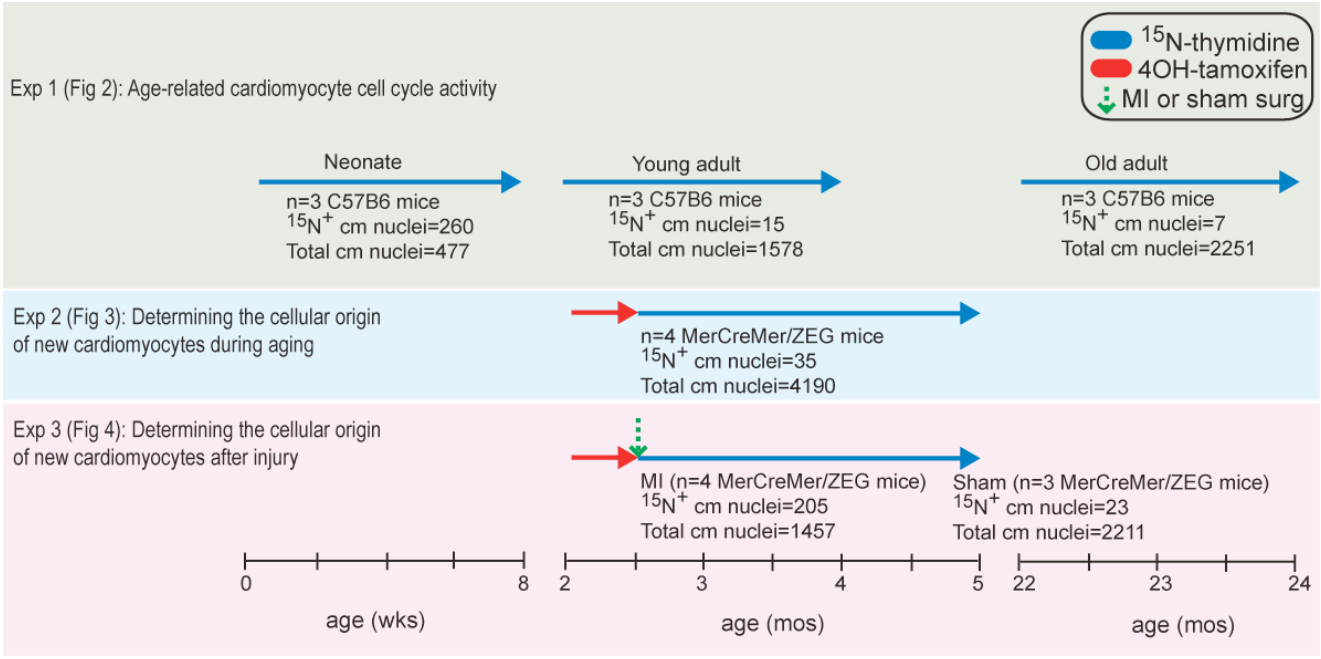

Figure S2: Labeling protocols.

Experiment1:

- Neonate: labeling started at post-natal day4. ^{15}N-thymidine (50µg/g) administered by twice-daily subcutaneous injection until mice were 4 wks-old. Then osmotic minipumps were implanted subcutaneously for 4 additional wks (20µg/hr).
- Young and old adults: ^{15}N-thymidine delivered continuously by subcutaneous osmotic minipump for 8wks (20µg/hr).

Experiment 2:

- 4OH-tamoxifen was administered by daily intraperitoneal injection (0.5mg/day) for two weeks to 2mo-old MerCreMer/ZEG mice.
- ^{15}N-thymidine was then administered for 10 weeks via subcutaneous osmotic minipump (20µg/hr).

Experiment 3:

- 4OH-tamoxifen was administered by daily intraperitoneal injection (0.5mg/day) for two weeks to 2mo-old MerCreMer/ZEG mice.
- Mice underwent permanent ligation of the left anterior descending artery (myocardial infarction) or sham surgery.
- ^{15}N-thymidine was then administered for 8 weeks: 500µg bolus intraperitoneal at time of surgery followed by continuous delivery via subcutaneous osmotic minipump (20µg/hr).

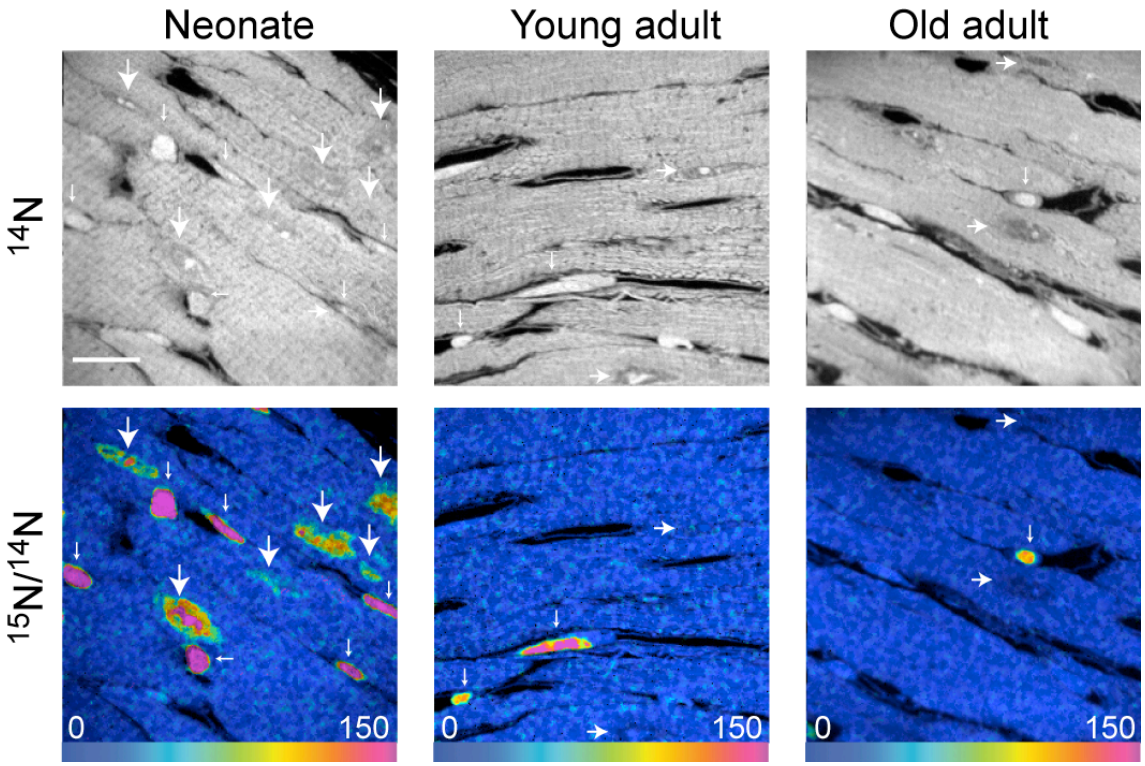

Figure S3: Cardiomyocyte DNA synthesis activity decreases with age. The early postnatal heart is characterized by robust DNA synthesis in cardiomyocytes and non-cardiomyocytes. In adulthood, DNA synthesis is observed primarily in non-cardiomyocytes. Cardiomyocytes with nuclear ^{15}N-labeling (large arrows), unlabeled cardiomyocyte nuclei (medium arrows), and labeled non-cardiomyocytes (small arrows). Scale bar = 20μm.

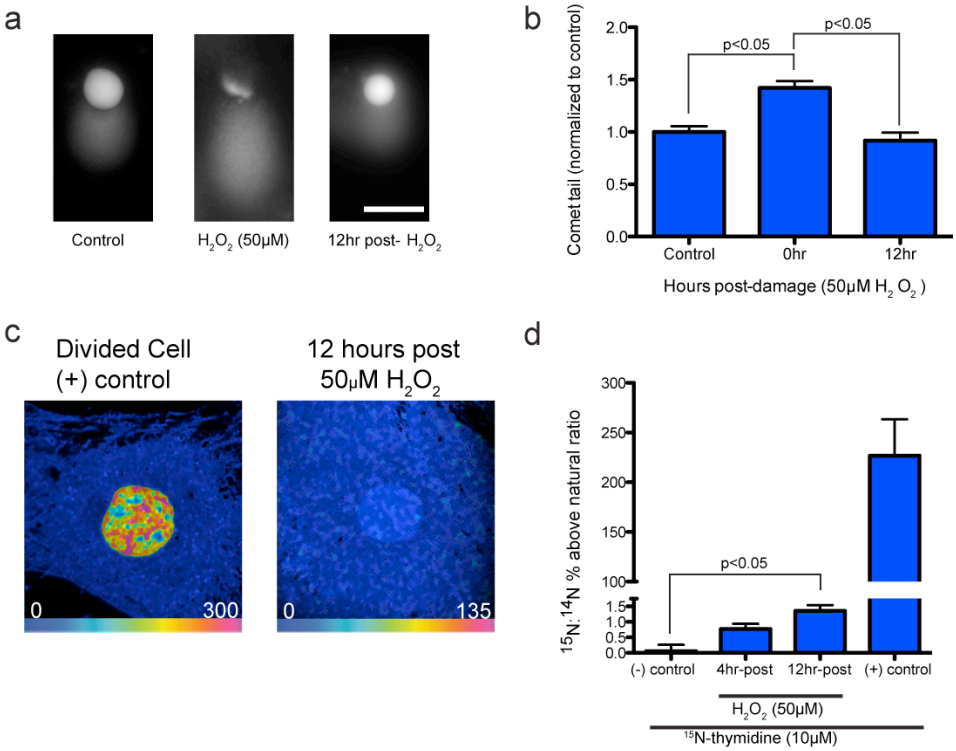

Figure S4: ^{15}N-thymidine incorporation after DNA damage cannot account for the level of labeling observed in cells completing the cell cycle.

a) Primary cardiac fibroblasts undergoing DNA repair. COMET assay demonstrates reproducible DNA damage with H_2O_2 exposure, followed by DNA repair[2]. Primary cardiac fibroblasts were grown to confluence, then serum starved. Cells were exposed to H_2O_2 (50 μM) for 30 minutes after which the cells were maintained in medium containing 10% fetal bovine serum. Immediately after DNA damage, extensive DNA streaking is observed, consistent with DNA damage. After removal of H_2O_2 and addition of serum containing medium, DNA streaking resolves consistent with DNA repair. Scale bar = 40μm.

b) Bar graph depicting quantitative results of COMET assay from (a). Tails (representing streaking damaged DNA) were measured and normalized to control tail length. An increase in the tail length is observed immediately after exposure to H_2O_2, which normalized within 12hrs, consistent with DNA repair. Mean ± S.E.M. One-way ANOVA

c) MIMS images of cells undergoing DNA repair. Image to the left demonstrates positive control cell that has undergone division in medium containing the same concentration of ^{15}N-thymidine (10μM). To the right is an image of fibroblast exposed to ^{15}N-thymidine for 12hrs after exposure to H_2O_2 (50μM).

d) Quantitative analysis of mean nuclear ^{15}N-labeling suggests low-level incorporation of ^{15}N-thymidine by fibroblasts after exposure to H_2O_2 (50μM). This low-level labeling is approximately 2 orders of magnitude below that observed in dividing cells, exposed to the same concentration of ^{15}N-thymidine. The absence of intense ^{15}N-thymidine incorporation, even after supraphysiologic doses of H_2O_2, is expected given that the scale of base replacement during repair after strand breaks presumably represents only a small fraction of the total nucleotides comprising the genome[3,4]. Moreover, DNA breaks tend to preferentially occur at base pairs that do not include thymidine[5,6]. Mean ± S.E.M. One-way ANOVA

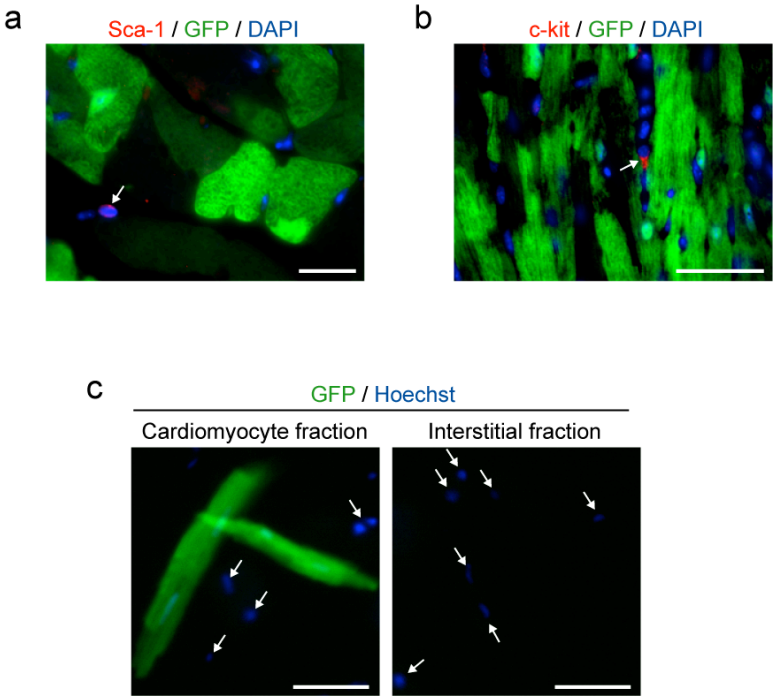

Figure S5: GFP is only detected in cardiomyocytes of MerCreMer^{+}/ZEG^{+} mice pulsed with 4OH-tamoxifen.

a) Sca-1-expressing cells in the heart are GFP^{-}. Immunofluorescent staining for GFP and sca1 in heart sections from MerCreMer/ZEG mice treated with 4-OH-tamoxifen. Scale bar = 40µm.

b) C-kit-expressing cells in the heart are GFP^{-}. Immunofluorescent staining for GFP and c-kit in heart sections from MerCreMer/ZEG mice treated with 4-OH-tamoxifen. Scale bar = 40µm.

c) Interstitial cells isolated from MerCreMer^{+}/ZEG^{+} mice did not express GFP. Hearts from MerCreMer/ZEG mice, treated with 4-OH-tamoxifen, were subjected to enzymatic digestion. Cardiomyocytes were separated from interstitial cells, plated, and treated with Hoechst. Approximately 80% of rod-shaped cardiomyocytes were GFP^{+}, whereas interstitial cells (white arrows) did not express GFP (n=1x10^{6} interstitial cells analyzed). Scale bar = 50µm. We conclude that if $^{15}N^{+}$ cardiomyocytes are derived from GFP-expressing progenitors in mammalian myocardium, the contribution is trivial.

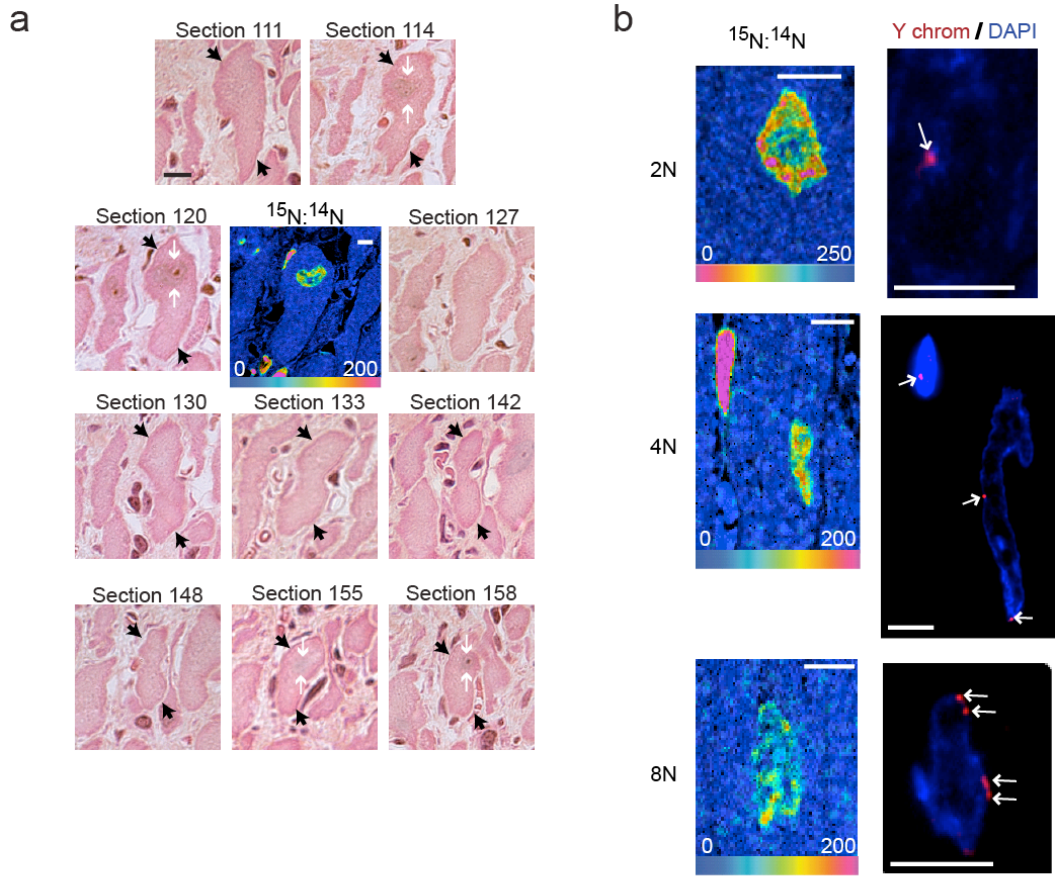

c

	^{15}N-labeled CM	Event #	Total analyzed	Frequency
Uninjured	Mononucleated	17	35	49%
	Diploid	22	34	65%
	Diploid/mono	6	35	17%
Sham	Mononucleated	4	14	29%
	Diploid	2	23	9%
	Diploid/mono	1	23	4%
MI	Mononucleated	46	117	39%
	Diploid	65	191	34%
	Diploid/mono	16	117	14%

Figure S6: DNA synthesis in cardiomyocytes is frequently associated with multinucleation and polypoidization.

a) Multinucleated cardiomyocyte. Trichrome staining was performed on serial adjacent sections. Selected images from one ^{15}N-thymidine labeled cardiomyocyte (black arrows) are shown. ^{15}N-labeled nucleus is observed in adjacent sections 120 and 114. ^{15}N-labeled nucleus is not observed in adjacent sections 127, 130, 133, 142, and 148. A second nucleus (white arrows) is observed in sections 155 and 158. Scale bar = 5μm.

b) Fluorescent *in situ* hybridization (Y-chromosome) demonstrating polyploidization of cardiomyocyte nuclei. Representative examples of diploid, tetraploid, and octoploid cardiomyocyte nuclei. Scale bar = 5μm.

c) Table summarizing the ploidy and multinucleation analysis of ^{15}N-thymidine labeled cardiomyocytes during normal aging (Fig 3, Supplemental Fig 2, Exp 2) and after

myocardial infarction (Fig 4, Supplemental Fig 2, Exp 3). The majority of cardiomyocyte DNA synthesis in the uninjured and injured heart occurred in polyploid (>2N) or multinucleated cardiomyocytes. This might be expected of myocardium in which the primary mode of increasing myocardial mass during normal aging or after injury was due to physiologic and/or compensatory hypertrophic growth.

a

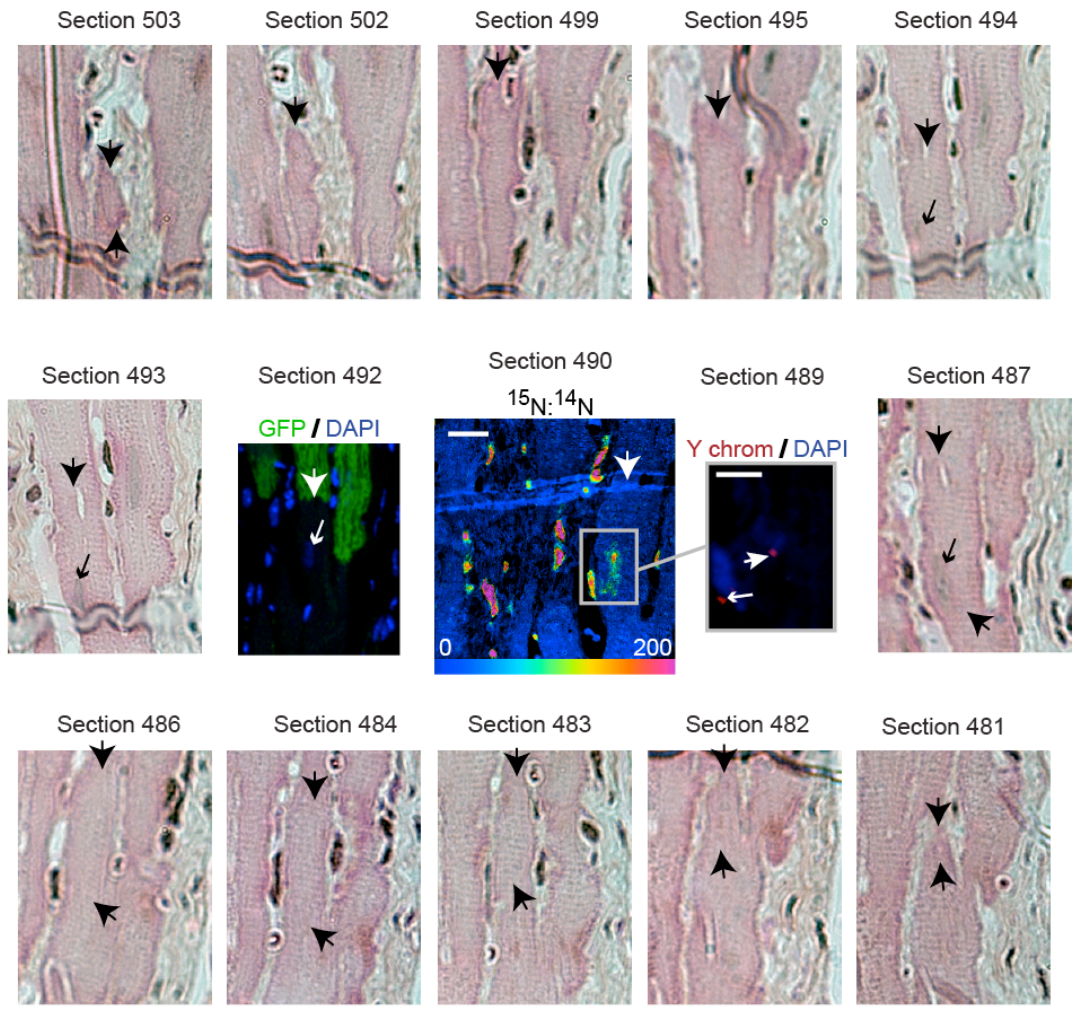

b

	Labeling	Total CM	$^{15}N^{+}$ CM	Diploid/Mono CM (%)
Uninjured	10 wks	4190	35	6 (0.14%*)
Sham	8 wks	2211	23	2 (0.09%)
MI border	8 wks	841	191	16** (3.2%)

**projected 0.75%/year*
***subset of 117 $^{15}N^{+}$ CM*

Figure S7: A minority of cardiomyocyte DNA synthesis results in new mononucleated, diploid cardiomyocytes.

a) New diploid mononucleated cardiomyocyte. Serial sections (0.5μm) were processed to determine the ploidy status, number of nuclei, and GFP expression of each ^{15}N-labeled cardiomyocyte (center). Left of MIMS HSI image: the $^{15}N^{+}$ nucleus (small arrow) is contained in GFP^{-} cardiomyocyte (large arrow) and is seen adjacent to two GFP^{+} cardiomyocytes. A majority of $^{15}N^{+}$ cardiomyocytes, however, were GFP^{+} (Figures 3,4), consistent with DNA synthesis occurring in preexisting cardiomyocytes. Right of MIMS HSI image: *in situ* hybridization demonstrates 1 Y-chromosome (diploid) in the $^{15}N^{+}$ cardiomyocyte nucleus (large arrow) and an adjacent interstitial cell (small arrow). Trichrome staining was performed in serial adjacent sections in both directions to define the

number of nuclei contained in the cell. Some of these images are shown here to illustrate the changing contours of the cell (large black arrows). The ^{15}N-labeled nucleus is identified (small black arrow), but disappears within a few sections. In contrast to the multinucleated myocyte (example shown in Supplemental Figure 6), no additional nuclei were observed. In this cardiomyocyte, which was sectioned longitudinally, the entire cell body was contained in 23 sections, 0.5μm each, suggesting a cross-sectional diameter of about 11-12μm.

b) Table showing the total rates of cardiomyocyte DNA synthesis and the percentage of that activity resulting in diploid, mononucleated cardiomyocytes. The projected annual rates of DNA synthesis and the generation rate of new diploid, mononucleated cardiomyocytes was similar in the uninjured adult mouse compared to sham-operated mice, but increased significantly in the region adjacent to the myocardial infarct (MI border).

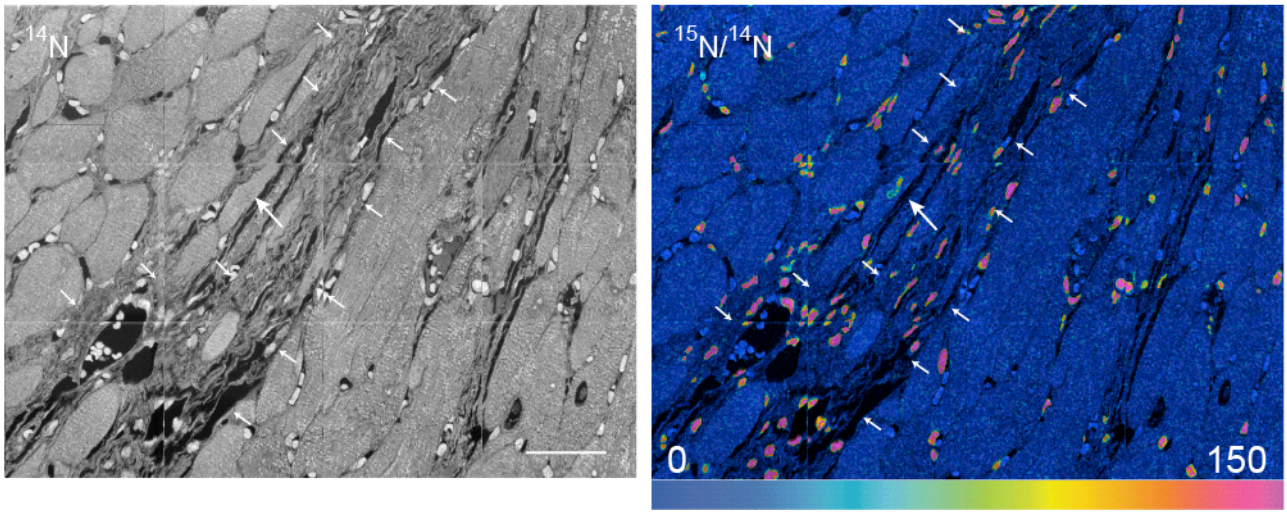

Figure S8: Cardiomyocyte DNA synthesis after myocardial infarction. Following injury, DNA synthesis frequency increases in cardiomyocytes. Mice were subjected to experimental myocardial infarction by ligation of the left anterior descending artery or sham surgery. Subcutaneous osmotic pumps were implanted to continuously label mice with ^{15}N-thymidine for 8 weeks following surgery. Right: ^{15}N:^{14}N HSI image demonstrates $^{15}N^{+}$ cardiomyocyte nuclei in the infarct borderzone (large white arrow) adjacent to the scar (small white arrows outline region of scar). Left: ^{14}N mass image in which the scar is visible (small white arrows). Mosaic images assembled of 16 tiles, 60 μm per tile. Scale bar = 30μm.

a

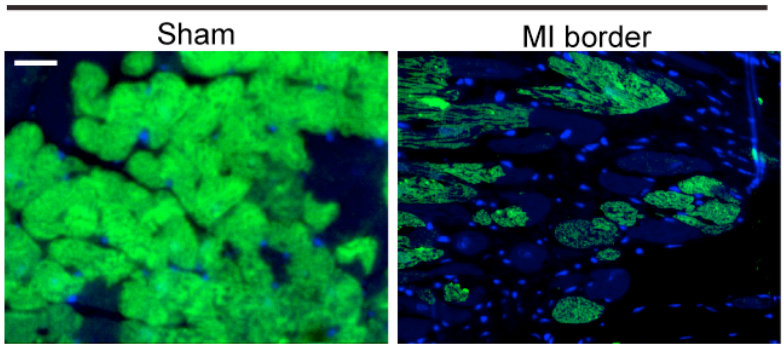

b

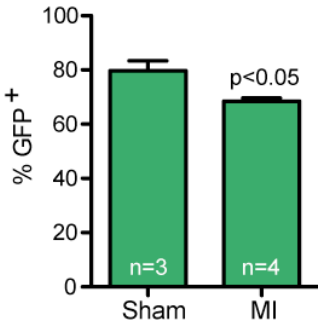

c

	Total counted	GFP$^+$	% GFP$^+$
Uninjured Adult	1111	933	83%
$^{15}N^+$ CM	35	27	77%
Polyploid CM	12	10	83%
Diploid CM	22	17	77%
Multinucleated CM	18	14	78%
Mononucleated CM	17	14	82%
Diploid/Mono CM	6	5	83%
Sham	3411	2693	79%
$^{15}N^+$ CM	23	19	83%
Polyploid CM	21	18	86%
Diploid CM	2	1	50%
Multinucleated CM	10	8	80%
Mononucleated CM	4	3	75%
Diploid/Mono CM	1	0	0%
MI	7063	4766	67%
$^{15}N^+$ CM	205	146	71%
Polyploid CM	126	97	77%
Diploid CM	65	47	72%
Multinucleated CM	59	42	71%
Mononucleated CM	41	29	71%
Diploid/Mono CM	16	11	69%

Figure S9: Myocardial infarction leads to a dilution of the GFP$^+$ cardiomyocyte pool at the infarct borderzone.

a) Immunofluorescent images of GFP-stained sham versus MI (borderzone-scar on the right) histologic sections of the left ventricle. Table showing the total rates of cardiomyocyte DNA synthesis and the percentage of that activity resulting in diploid, mononucleated cardiomyocytes. The rates of DNA synthesis and the generation rate of new diploid, mononucleated cardiomyocytes was similar in the uninjured adult mouse compared to sham-operated mice, but increased significantly in the region adjacent to the myocardial infarct (MI border).

b) Bar graph depicting the percentage of GFP$^+$ cardiomyocytes in the left ventricle of sham operated mice versus the infarct border region of mice after experimental myocardial infarction. Data expressed as the mean percentage of GFP labeled myocytes ± s.e.m.

c) Tabular analysis in which myocytes have been pooled within each group of mice. In general, regardless of how the $^{15}N^+$ cardiomyocytes are parsed, they are predominantly GFP$^+$ consistent with DNA synthesis and division by preexisting cardiomyocytes. Note: due to the low number of analyzed diploid/mononucleated $^{15}N^+$ cardiomyocytes in the sham-operated group, the GFP analysis is underpowered to determine origin of the cells. However, with the exception of the diploid/mononucleated pool (in which 0/1 cells expressed GFP) the overall numbers are similar to the uninjured heart.

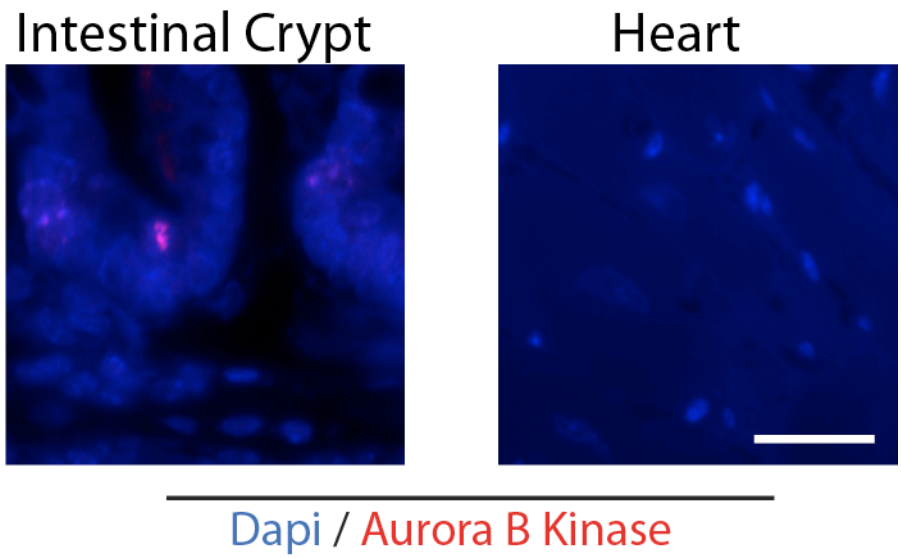

Figure S10: Aurora B Kinase is not detectable in ^{15}N-thymidine labeled cardiomyocytes 8 weeks after injury or in uninjured hearts. Left: Positive control demonstrating aurora B kinase staining of mitotic cells in the crypt of the small intestine. Right: Aurora B kinase positive cardiomyocytes were not detected in the infarct borderzone 8 weeks after myocardial infarction, including in the ^{15}N-thymidine labeled myocyte nuclei (one of which is included in this field). Similar findings were observed in uninjured or sham operated hearts. Cells that completed cytokinesis at some point in the preceding 8 wks (the $^{15}N^{+}$/diploid/mononucleated population) would no longer be expected to express aurora B kinase and thus the absence of aurora B kinase staining is not surprising given the low frequency of observed such new cardiomyocytes in either the uninjured or injured hearts (Figs 3-4, Supplemental Fig 7). Scale bar = 20μm.

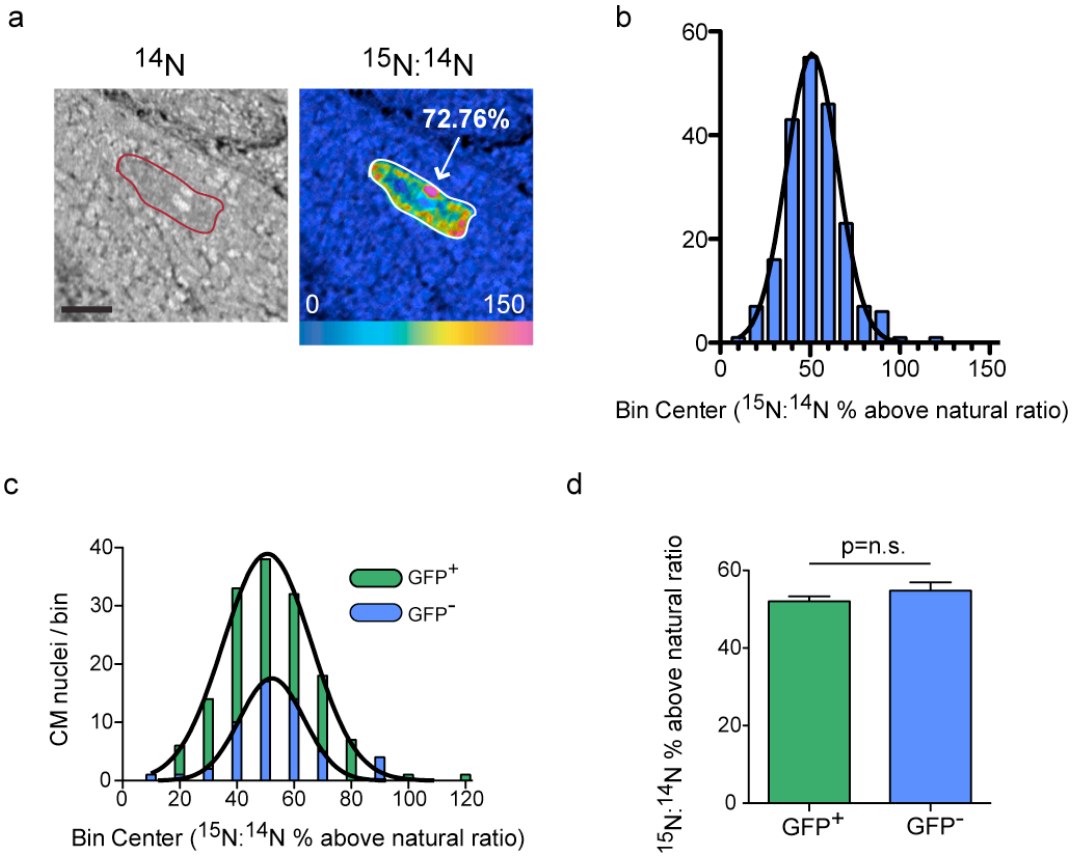

Figure S11: MIMS quantitative analysis of ^{15}N-thymidine incorporation by cardiomyocytes suggests a single round of DNA synthesis after myocardial infarction.

a) Left**:** ^{14}N image demonstrating cardiomyocyte sarcomeric structures surrounding cardiomyocyte nucleus (left red outline). Right**:** Corresponding HSI ratio image demonstrating ^{15}N-signal localized to cardiomyocyte nucleus. The number denotes the mean ^{15}N:^{14}N% above natural abundance for all pixels contained within the outlined nuclear region. Quantitation of nuclear ^{15}N-labeling was performed by tracing the nuclei of all ^{15}N-labeling cardiomyocytes. Scale bar = 5μm.

b) Histogram plotting the results of quantitative analysis of mean nuclear ^{15}N-labeling of ^{15}N^{+} cardiomyocytes (Gaussian fit line R^2=0.99). ^{15}N-labeled cardiomyocyte nuclei are distributed in a single normally distributed population (KS normality test=pass). Replication of the genome in the presence of ^{15}N-thymidine results in labeling of all newly synthesized DNA strands, while the preexisting template strands are unlabeled. With each additional round of DNA replication in the presence of ^{15}N-thymidine, a higher relative number of the total DNA strands will be ^{15}N-labeled. Thus, if a subset of divided cardiomyocytes underwent a second round of DNA synthesis, we would have expected a second population with a higher level of ^{15}N-labeling.

c) Histogram plotting mean nuclear ^{15}N-labeling of GFP^{+} (green bars) versus GFP^{-} (blue bars) cardiomyocytes. Both types of cardiomyocytes are contained in similar normally distributed populations. GFP^{+}: KS normality test=pass, Gaussian fit line R^2=0.99. GFP^{-}: KS normality test=pass, Gaussian fit line R^2=0.96.

d) Bar graph comparing mean nuclear ^{15}N-labeling of the GFP^{+} and GFP^{-} populations shown in (c). There is no significant difference ($p>0.05$) in the level of ^{15}N-labeling. Mean ± S.E.M.

Supplement References

1 Nikolova, V. *et al.* Defects in nuclear structure and function promote dilated cardiomyopathy in lamin A/C-deficient mice. *J Clin Invest* **113**, 357-369 (2004).

2 Olive, P. L. & Banath, J. P. The comet assay: a method to measure DNA damage in individual cells. *Nat Protoc* **1**, 23-29 (2006).

3 Bergmann, O. *et al.* Evidence for cardiomyocyte renewal in humans. *Science* **324**, 98-102 (2009).

4 Kajstura, J. *et al.* Cardiomyogenesis in the adult human heart. *Circ Res* **107**, 305-315 (2010).

5 Alberts, B., Wilson, J. H. & Hunt, T. *Molecular biology of the cell*. 5th edn, (Garland Science, 2008).

6 Dinant, C., Houtsmuller, A. B. & Vermeulen, W. Chromatin structure and DNA damage repair. *Epigenetics Chromatin* **1**, 9 (2008).